INTERNATIONAL CONFERENCE ON LIGHTNING PROTECTION
33rd International Conference on Lightning Protection
25 - 30 September 2016
Estoril, Portugal

On the positive upward leader in response to downward stepped leader in a 10m rod-to-rod long air gap

Hengxin He, Junjia He, Xiangen Zhao
State Key Laboratory of Advanced Electromagnetic Engineering and Technology
Huazhong University of Science and Technology
Wuhan, China
hengxin_he@hust.edu.cn

Weijiang Chen
State Grid Corporation of China
Beijing, China
weijiang-chen@sgcc.com.cn

Franco' D Alessandro
PhysElec Solutions
Hobart, Australia
info@physelec.com

***Abstract*— Long negative sparks have been widely used to investigate the lightning attachment process of grounded structures. The rod-to-rod air gap is one of the most common configurations used in laboratory experiments to investigate the characteristics of the positive upward leader in response to the negative descending leader steps. In the research presented in this paper, experimental observations have been carried out in a 10 m rod-to-rod air gap. Many discharge parameters were recorded using a high speed camera, wideband current measurement devices and Pockels electric field sensors. It was found that the average linear charge density of a negative leader is about 142.2μC/m, which is close to the charge density of a natural lightning downward leader delivering a stroke current of about 7kA. The maximum upward streamer and leader lengths are 2.24 m and 0.64 m, respectively. The space E-field E_n in negative long sparks consists of a series of electric field steps. Although the dE_n/dt is relatively high during the formation of each negative leader step, the dE_n/dt decreases significantly and the upward leader stops elongation during the time interval of two negative leader steps. As a consequence, the velocity and length of the upward leader initiation by negative long sparks might only be close to the initiation stage under natural lightning conditions.**

Keywords-lightning attachment; negative long spark; negative stepped leader; positive upward leader; streamer; velocity; current; electric field; linear charge density;

I. INTRODUCTION

Lightning strikes and the consequent electromagnetic effects frequently cause unscheduled interruptions of modern electrical and electronic system. Compared with artificially-triggered lightning and field observation techniques, a simulated electrical discharge in a laboratory is more controllable and reproducible and hence provides an alternative way to study lightning shielding issues. From a phenomenological viewpoint, it is believed that some similarity exists between negative cloud-to-ground flashes and negative long air gap discharges. Therefore, negative long sparks have been widely used to investigate the lightning attachment process of grounded structures [1-3].

The rod-to-rod air gap is one of the most common configurations used in laboratory experiments to simulate lightning attachment. The upper rod is stressed with a negative impulse voltage to simulate the descending leader. A grounded rod launches a positive upward streamer or connecting leader in response to the dynamic field produced by the descending leader. Using this experimental setup, it is not only possible to obtain the breakdown characteristics of the air gap, but it also helps to investigate the strike probability of test objects by changing the location of upper or lower rods. Key issues of study in these experiments are the characteristics of upward connecting leaders emerging from the grounded rod. It is of great significance to acquire physical parameters of the upward connecting leader, which can extend our knowledge regarding the lightning attachment mechanism.

Using a 3.5m rod-to-rod air gap, Suzuki [4] proposed a scale model test under negative lightning and switching impulse voltages, respectively. According to the streak photographs, there was not enough space for the negative stepped leader to form. The air gap was bridged by streamers in several microseconds. The velocity of a connecting leader is up to ~10^5 m/s during the final jump. Hence, breakdown of the gap in the aforementioned study did not involve leader attachment processes. The physical breakdown process of a 7 m rod-plane gap under negative switching impulse was recorded by the Les Renardières Group [5]. It indicated that there would be two or three negative descending leader steps before the final jump. Later, the breakdown performance of a 16.7 m air rod-plane gap subjected to negative switching impulses was observed by Ortega and coworkers [6]. They found that the average number of leader steps was about five in such a gap configuration. It inferred that the typical negative leader parameters for longer gaps begin to approximate natural lightning downward stepped

leaders with a low-amplitude return-stroke current. In order to revise the EGM models and investigate the lightning shielding failure of UHV double-circuit transmission lines, more experiments have been carried out in [1] and [7] by using negative long sparks. However, there were no further data available regarding the positive upward leader in response to negative descending stepped leaders.

D'Alessandro et al carried out an experiment to examine the shielding performance of a 5 m tall Franklin rod by using a 26 m air rod-plane gap [2]. The positive upward leader image incepted from grounded rod was clearly recorded by an ICC camera. But the physical parameters of the upward leader were not reported in the literature. Recently, positive upward leaders emerging from horizontal conductors have been studied in [8]. A plane electrode with a rod installed at the symmetry axis was adopted as an upper rod, and the minimum distance between rod tip and conductors was 6 m. From the recorded high speed images, there was only one negative descending leader step formed before breakdown. Combined with measured current waveforms, the velocity and charge density of positive upward leaders in response to the single negative leader step were presented.

The aim of this paper is to investigate the characteristics of positive upward leaders in response to multiple negative descending leader steps. A rod-to-rod air gap was adopted with a length of up to 10 m. Firstly, a synchronized observation system was established including a high speed camera, wideband current measurement devices and Pockels electric field sensors. Secondly, the positive upward leader initiated from the grounded rod in response to the negative stepped leader was observed in a 10 m rod-rod air gap. The effect of the electric field due to the negative stepped leader on the propagation of the positive upward leader was analyzed. The key features of upward leaders initiated by negative long sparks in the laboratory and natural lightning are compared. The experimental data presented here canprovide a reference for improving the lightning simulation test method and lightning attachment simulation models.

II. EXPERIMENTAL SETUP

A. Experimental Apparatus and Procedure

Experiments were conducted at the outdoor impulse test yard of the ultra-high voltage AC test base of China in Wuhan. The gap configuration was a traditional rod-to-rod gap, as illustrated in Fig. 1. The vertical distance between the upper rod and grounded rod, *D,* was 10 m, and the height of grounded rod was 4.5 m.

The tip of the upper rod electrode was hemispherical with a diameter of 2 cm. The length of upper rod body was 10 m. The grounded rod electrode was made of steel and cylindrical in shape, with a cross-sectional area of 36 cm^2. At its tip was a copper sphere with a radius of 6 cm. The height from the lower rod tip to the ground plane, *h,* was 4.5 m. The ground plane electrode was a 20×20 m iron plate placed on a 50 x 50 m steel mesh.

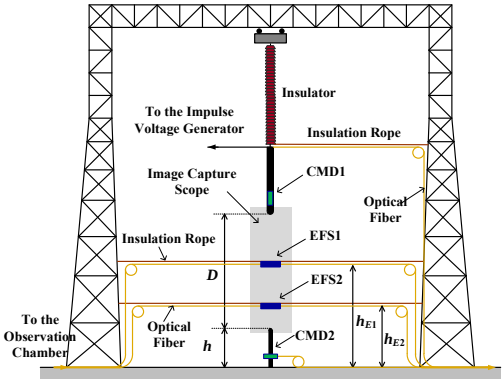

Figure 1. The sketch of the experimental configuration.

All the experiments were carried out using a 25-stage impulse voltage generator with a maximum voltage output of 7.5 MV. The 50% breakdown voltage of a rod-plane air gap subjected to negative switching impulses varies for different time-to-crest values of the voltage waveform, described by classical U-shaped curve. The critical time-to-crest $T_{cr,}$ corresponding to a critical impulse voltage shape, defines the minimum breakdown voltage $U_{50\%(critical)}$. According to the experimental results published in [6], T_{cr} of a rod-plane air gap subjected to negative switching impulses can be expressed as a function of the gap length *D,* given by:

$$T_{cr} = 10D \tag{1}$$

with T_{cr} in microseconds and D in meters. The $U_{50\%(critical)}$ related to the gap length to D can be determined by the empirical formula:

$$U_{50\%(critical)} = 1.18D^{0.45} \tag{2}$$

with $U_{50\%(critical)}$ in MV and D in meters. For a 10 m air gap, these formula give T_{cr} = 100 μs and $U_{50\%(critical)}$ = 3.3 MV. In consideration of the actual conditions of the generator, the wave front time was set to about 80 μs in the present study. The peak value of the applied impulse was controlled in the range of 3.8-4.0 MV for the rod-rod gap. As a consequence, the breakdown probability is greater than 0.5 but smaller than unity. The impulse voltage was measured by a capacitive divider with an accuracy of ±0.5%. During the experiment, the temperature and relative humidity varied in the range of 17℃ to 22℃ and 75% to 85%, respectively. Twenty discharges were recorded in total.

The arrangement of discharge electrodes and observation sensors is shown in Fig. 1. The discharge current of the upper rod electrode and the grounded rod are recorded by the current measurement devices CMD1 and CMD2, respectively. CMD1 was embedded in the body of the upper rod (described further in the following section). CMD1 and CMD2 signals were fed back to the control room via optical fiber fixed with insulating ropes.

Two electric field sensors (EFS1 and EFS2) were located on the central axis. EFS1 was used to record the vertical electric field variation at the mid-point of the upper and lower rod electrodes. EFS2 was used to record the vertical electric

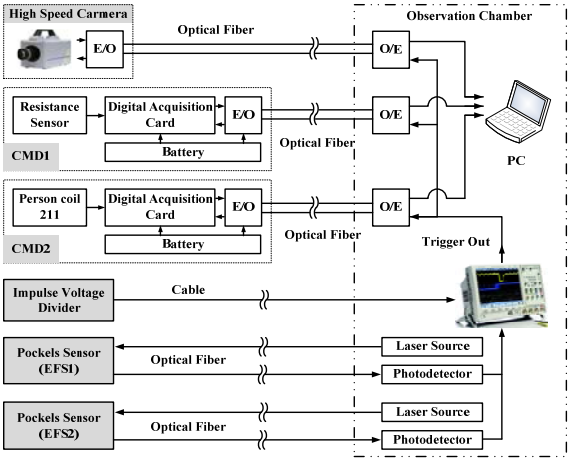

Figure 2. The schematic diagram of the synchronized observation system.

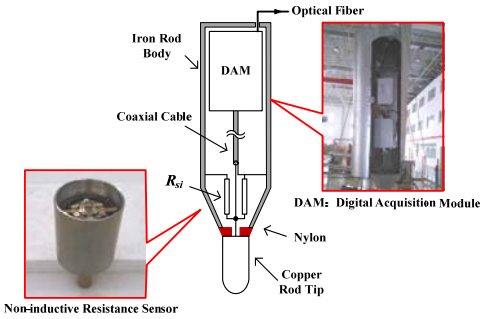

Figure 3. The structure of the current measure device integrated with the high potential electrode.

field variation above the grounded rod, i.e., in the region where an upward leader if formed. The heights of the field sensors, h_{E1} and h_{E2}, were set to 5.5 m and 8.5 m, respectively. The sensors and connecting optical fiber cable were fixed with insulating ropes.

A Photron Fastcam SAX high speed camera (HSC) was employed to record the leader propagation image. The capture parameters of this high speed camera in the present study were set to 300 kfps (kilo-frames per second), 256×48 pixels of resolution, and 1/300 ms shutter speed. The field of view of the high speed camera is shown as the gray rectangular area in Fig. 1. All of the experiments were carried out in the evening to ensure a good quality of recorded images.

The observation apparatus was synchronized according to the following procedure. The signal from the impulse voltage divider and photodetector output of EFS1 and EFS2 were fed to an oscilloscope (Tektronix DPO4104B-L) in the control room. The impulse voltage input signal was chosen to be the trigger reference signal of the oscilloscope. When the reference signal exceeded the trigger level, the oscilloscope was triggered. A triggered output TTL pulse was generated by the oscilloscope, which was used to trigger the current measurement device (CMD1 and CMD2) and high speed camera. The recorded images and current data were transmitted to a computer located in the control room via optical fiber. The logic diagram of the synchronized observation system is shown in Fig. 2. All signal transmission delays were corrected during the data processing stage.

B. Discharge Current Measurement Device

CMD1 was used to measure the discharge current profile at the high potential electrode, as illustrated in Fig. 3. In order to restrain the capacitive displacement current, the rod tip was insulated from the rod body using a thin nylon layer. One terminal of the resistance sensor was connected directly to the rod tip. The other end was connected to the rod body. This configuration ensured that the recorded signal only contains the discharge current i_d and the displacement current i_c flowing

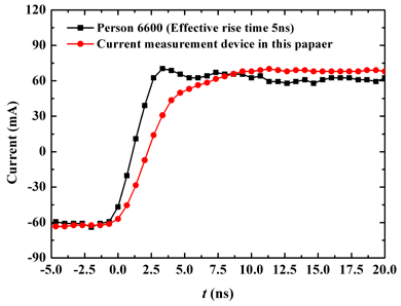

Figure 4. The square-wave response of the resistance sensor

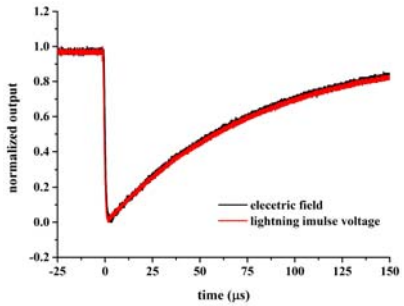

Figure 5. The response of the Pockels sensor in response to the standard lighting impulse

through the rod tip. The contribution of i_c can be neglected because the stray capacitance between the rod tip and grounded plane is negligibly small. The resistance sensor consisted of 12 inductance-free resistors in parallel with a total resistance value of 3.3 Ω. The square-wave response of the resistance sensor is shown in Fig.4. A Rogowski coil (Person 6600) was used as a standard sensor for comparison. It had an effective rise time of 5 ns. It can be inferred that the bandwidth of the resistance sensor is approximate 50MHz.

The output of resistance sensor was connected to the digital acquisition module (DAM) via a coaxial cable. The DAM consisted of a digital acquisition card, a photoelectric conversion unit and batteries which, shown in Fig. 2. The digital acquisition card was an Agilent U2702A with a sampling rate of 500MHz. The recorded data was transmitted to the host computer immediately after the DAM was triggered.

For convenience of installation, the current sensor of CMD2 was a Rogowski coil (Person 411) with a bandwidth of

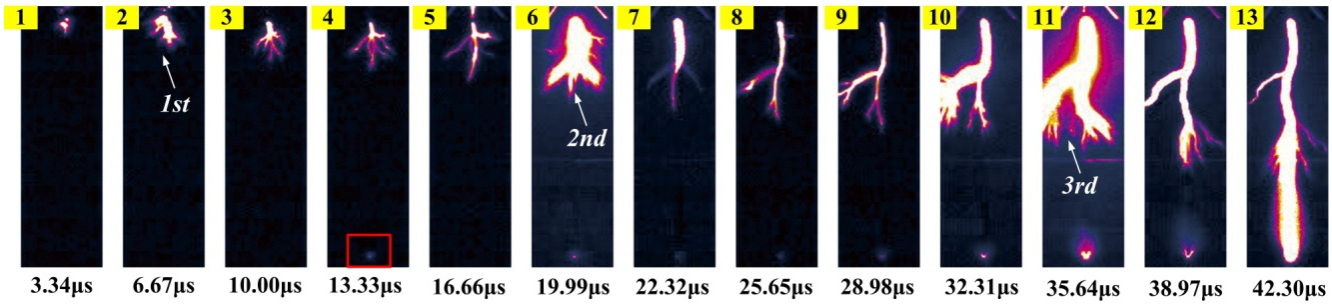

(a) High speed images

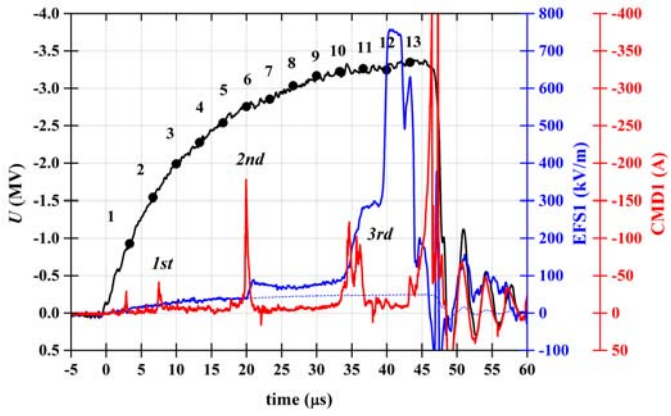

(b) Upper rod

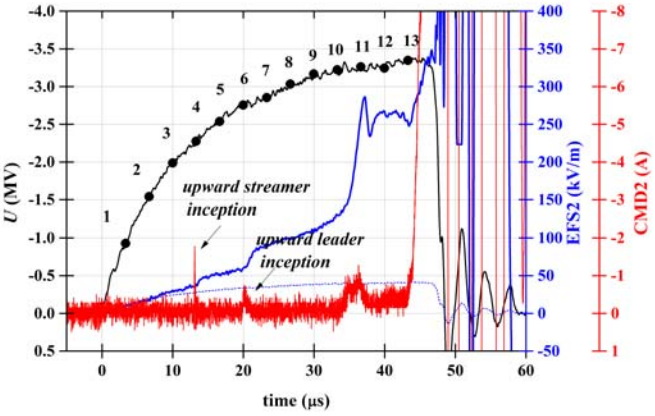

(c) Grounded rod

Figure 6. The observed discharge images, current waveforms, electric field waveforms and impulse voltage waveforms for both upper and grounded rod during the breakdown process.

0.5-20 MHz. It was installed on the ground (earthed) wire of the lower rod. The output signal of the Rogowski coil was acquired by the DAM locally and transmitted to the host computer via optical fiber.

C. *Pockels electric field sensor*

There are two kinds of Pockels sensors that can be used to measure the Poissonian electric field in long air gap discharges. The first one is named an "integrated electric-optic sensor" (IEOS) [9]. It has the advantage of being small in size due to its integrated circuit ("chip") design. This sensor was utilized to measure the Poissonian field near the edge of the space charge zone produced by positive streamer discharges. However, this kind of Pockels sensor is often integrated with a metal antenna and electrode in order to modulate the measured electric field signal and increase the sensitivity. The electric field produced by the negative stepped leader is greater than the field produced by positive streamer discharges. The former may reach 1 MV/m or more. If the IEOS is exposed to such a lareg field, a bi-leader discharge may emerge from the floating metal electrode and destroy the sensor chip.

Based on a discrete optical component concept, a transient electric field sensor was developed using a BGO crystal. The fundamental principle of this kind of Pockels sensor can be found in [10]. A light beam from the optical source travels through a polarizer and a quarter-wave plate. It is decomposed into two components of perpendicular polarization directions. When they pass through the BGO crystal, a phase shift occurs between the two components. The degree of the phase shift is related to the applied electric field strength E_a, which can be described by the intensity of the emerging beam I_{out}. I_{out} can be detected by the photodetector which is linear with E_a in a certain range.

In the present study, the BGO crystal length was 2 cm with a highly-sensitive section of area 5×2 mm. All of the optical components and fiber terminals were encapsulated in a 6 cm long plexiglass tube with a diameter of 2 cm. The designed bandwidth of demodulator is in the range of 5 to 30MHz.The sensor was calibrated in the field created between two parallel plane electrodes subjected to a standard lightning impulse. The transient response of the sensor under the lightning impulse field is shown in Fig. 5. It can be seen there is good agreement between the voltage waveform and the response of the sensor. The calibration curve reveal good linear performance in the range of 50 to 800 kV/m.

III. OBSERVATION RESULTS AND DISSCUSSIONS

A. *Discharge phenomenon before the final jump*

The typical phenomenon and electrical parameters of streamer-leader propagation in the 10 m rod-to-rod air gap observed is shown in Fig. 6.

From the recorded high speed images shown in Fig. 6 (a), there were three negative descending leader steps before the final jump. Combined with the measured current waveform at the upper rod by CMD1, shown by the red curve in Fig. 6(b), the initiation time for each stepped leader was 7.49μs, 19.8μs and 34.5μs, respectively. For a negative leader step without branching, the corresponding current waveform had single peak pulses at t=7.49μs and 19.8μs. Serving as a contrast to the single filament situation, the current waveform would have two peak values when the negative stepped leader has two branches at t=34.5μs. It might be caused by the inception time delay of leader branches. The peak current at each leader step was -38.3A, -178.5A and -121.9A.

Positive upward streamer inception occurred at t = 13.1μs, seen as a narrow pulse current with a width of less than 120 ns. There were no optical phenomena observed before the second negative descending leader step was formed. The positive upward leader was initiated from the grounded rod at t = 19.8μs in response to the second descending leader step. The peak value of the corresponding current pulse was about 0.68 A. The extension of the positive upward leader was very slow between the time interval of the second and third downward leader steps. The light intensity of the upward streamer-leader zone also became weaker. At the time of the third negative descending leader step at t = 34.5μs, the positive upward streamer zone had a grown considerably. The upward leader channel also produced two branches and the light intensity of leader channel behind the streamer zone was as bright as the negative downward leader channel. After the conjunction of the upward streamer and downward leader branches at t= 42.3μs, the final jump took place, followed by a large increase in the discharge current. The breakdown voltage of this discharge was 3.34 MV.

According to the measured electric field waveform, shown by the blue curves in Figs. 6(b) and (c), there was a significant step rise in the time domain in response to the formation of each downward leader step. For the vertical E-field waveform in the middle of the air gap recorded by EFS1, the field was almost constant between the two electric field steps, for the time interval between two leader steps. It was found that the critical ambient field (treated as the vertical E-field in the middle of the air gap) for upward streamer and upward leader inception is about 35.8 kV/m and 83.2 kV/m, respectively. The value of vertical E-field reached 752 kV/m before the final jump took place, but this might be because the location of EFS1 was close to the tip of negative downward leader after t = 35.64 μs. From the vertical E-field waveform above the grounded rod tip recorded by EFS2, the E-field intensity also increased in a step-like manner. For t > 34.5 μs, the E-field value of EFS2 was approximately constant at around 250 kV/m to 300 kV/m. this may have been because the EFS2 sensor was surrounded by the positive upward streamer after the formation of the third downward leader step.

B. Statistical features of negative stepped leader

Based on the aforementioned results, it appears that the inception and propagation of the upward leader is closely related to the behavior of the negative, downward, stepped leader. The statistics obtained for the negative stepped leader from 20 discharges are presented in Table I.

TABLE I. STATISTICAL FEATURES OF THE NEGATIVE STEPPED LEADER

Number of downward leader steps	3.8±1.2
Time interval between two leader steps (μs)	12.9±6.0
Average length of a single leader step (m)	1.5±0.7
Average final jump length (m)	4.2
Average peak current for each leader step (A)	-117.8±66.6
Average injected charge volume of a single leader step (C)	-80.9±53.6
Average charge density (μC/m)	142.2±97.6
Average velocity of stepped leader (cm/μs)	13.6±8.8
Average E-field peak value of EFS1 (kV/m)	-774.5

C. Discharge parameters of positive upward leader

The discharge parameters of the positive upward streamer-leader system have been derived, including the upward streamer inception time t_s, the continuous upward leader inception time t_i, the average duration of continuous upward leader propagation t_d, the maximum upward streamer length before the final jump L_s, the maximum upward leader length L_l before the final jump, and the average velocity of the upward leader v_L, The statistics derived are presented in Table II.

The parameter t_s was identified according to the current waveform of grounded rod shown in Fig. 6(b). If the streamer current pulse was not captured, e. g., due to the limited bandwidth of the Person coil, t_s was obtained from the high speed optical image. In Fig. 6(a), t_s was equal to 13.33μs. The difference between the two data processing methods was found to be minimal. The average upward streamer inception time was 12.0μs with a variance of ±2.5μs. t_s is quite stable because the upward streamer inception depends mostly on the Laplace E-field produced by the negative impulse voltage.

The parameter t_i was obtained in a similar way, as it often corresponded to the second or third descending leader formation time. The average upward leader inception time was 25.5 μs with a variance of ±7.9 μs. The spread in this parameter is close to the time interval of the negative descending stepped leader. It indicates that the initiation of a continuous upward leader is driven by the Poissonian E-field of the descending stepped leader.

TABLE II. DISCHARGE PARAMETERS OF POSITIVE UPWARD LEADER

t_s (μs)	12.0±2.5
t_i (μs)	25.5±7.9
t_d (μs)	39.4±18.9
L_s (m)	1.6±0.6
L_l (m)	0.64±0.3
v_L (cm/μs)	1.75±0.6

The maximum length of the upward streamer and leader before the final jump was obtained from high speed images. The average value of L_l was only 0.64 m. Considering also the upward streamer zone, the axial length of the positive upward streamer-leader system was 2.24 m at the time of the final jump. About 78% of the air gap was spanned by the negative descending stepped leader. It indicates that the continuous

upward leader cannot grow to long lengths, even in a 10 m air gap.

The average upward leader velocity was 1.75 ± 0.6 cm/μs. This value is close to the leader velocity of 1.5 cm/μs obtained from traditional rod-plane gap investigations under positive switching impulses. From recorded high speed images such as the one shown in Fig. 6(a), the propagation of the upward leader almost stopped in the time interval between two negative leader steps. Although more negative space charge was injected into the air gap as the stepped leader approached, the corresponding vertical E-field rises in a step-like manner. The E-field rise time is approximately equal to the pulse width of stepped leader current pulses. Furthermore, it remains almost constant during the time interval between two negative descending leader steps, as shown in Fig. 6(b). The relationship between the upward leader velocity and Poissonian E-field induced by the downward stepped leader is discussed in the next section.

D. Discussion of results in comparison with natural lightning attachment process

The observed discharge parameters of negative stepped leaders in the present study are consistent with the results in [2] and [6]. The average charge density ρ_n of a negative leader is 100-130 μC/m for a 16.7 m rod-plane air gap, and 70-100 μC/m for an air gap of 26-31 m, compared to 142.2 ± 97.6 μC/m in our present study. According to Dellera's work in [11], the relationship between charge density q_n and return stroke current I deduced from field observations is given by:

$$q_n = 38 \times I^{0.68} \tag{3}$$

where q_n is in μC/m and I is in kA. The corresponding return stroke current is 7.0 kA for a q_n of 142.2 μC/m. This result implies the charge density of the stepped leader generated in the laboratory per the setup described in this paper is close to that of a natural lightning discharge of about 7 kA.

If the H.V. electrode is stressed with a standard double-exponential impulse voltage $U(t)$, the Laplacian E-field E_L in the gap varies with time as shown by the red curve (a) in Fig. 7. As analyzed earlier, the space E-field E_n in response to the negative stepped leader is comprised of a series of steps, as shown by the green curve (c) in Fig. 7. The number of electric field steps is approximately equal to the number of negative leader steps. The ΔE of each electric field step is related to the corresponding charge density and geometric position of negative leader step. However, the E-field waveform E_b produced by a natural, negative, descending leader rises in a monotonically exponential manner as shown by the blue curve (b) in Fig. 7. This difference may be due to the fact that the downward leader can have multiple branches as well as leader steps, rather than simply two or three leader steps in a long negative spark.

In reference [12], the positive leader velocity v_L not only depends on the gap E-field intensity E but also on the E-field rise rate dE/dt, given by:

$$v_L = k_1 E + k_2 \frac{dE}{dt} \tag{4}$$

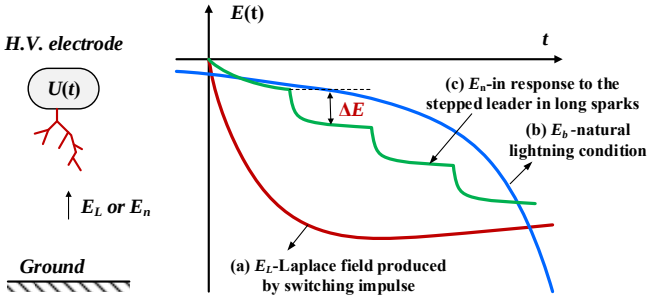

Figure 7. Illustration of space electric field due to negative long sparks and under natural lightning conditions.

where the coefficients k_1 and k_2 are related to the gap configuration and applied voltage waveforms.

In the natural lightning attachment process, the E-field rise rate dE_b/dt keeps increasing for ~10 ms after positive upward leader inception. As a consequence, the leader velocity can vary from ~10^4 m/s up to ~10^5 m/s. Furthermore, field observations show that the length of positive upward leaders can extend up to 100 m or more. For long negative sparks in the laboratory, although the dE_n/dt is relatively high during the formation of each negative leader step, it normally only lasts for several μs. This is why upward leader propagation always occurs at the rising front of each E-field step observed in this paper. When dE_n/dt decreases significantly, the upward leader stops propagating, i.e., during the time interval between two negative leader steps. As a result, the velocity and length of the upward leader might only be close to the initial stages of natural lightning discharges. In order to get the upward leader velocity with a higher accuracy, a more effective observation techniques such as LAPOS [13] must be introduced in further works.

IV. CONCLUSION

The characteristics of positive upward leaders in response to multiple negative descending leader steps has been investigated in a HV laboratory. A 10 m rod-to-rod air gap was adopted and discharge parameters were recorded using a high speed camera, wideband current measurement devices and Pockels electric field sensors. The effect of the electric field due to the negative stepped leader on the propagation of positive upward leaders was analyzed. The difference between the upward leader developed from long negative sparks in the laboratory and practical (natural) lightning was compared. The outcomes of the analysis can be summarized as follows:

- The average number of negative downward leader steps is about 3.8 in the 10 m rod-to-rod air gap. The average charge density ρ_n of the negative leader is 142.2 μC/m, which is close to the charge density of a natural lightning downward leader delivering a stroke current of about 7 kA. The average velocity of the stepped leader was found to be about 13.6 cm/μs.
- Upward streamer inception appears to be mainly dependent on the Laplacian E-field due to negative impulse voltage produced. The streamer inception time

is 12.0 ± 2.5 μs. The initiation of a continuous upward leader is driven by the Poissonian E-field due to the descending stepped leader. The maximum upward streamer and leader length are 2.24 m and 0.64 m, respectively. The continuous upward leader does not propagate a significant distance, even in air gaps of length up to 10 m.

- The space E-field E_n in negative long sparks consists of a series of electric field steps. Although the dE_n/dt is relatively high during the formation of each negative leader step, the dE_n/dt decreases significantly thereafter and the upward leader stops propagating between two negative leader steps. This aspect is different to the natural lightning attachment process. As a consequence, the velocity and length of upward leaders due to negative long sparks might only be close to the initial stages of the natural lightning attachment process.

ACKNOWLEDGMENT

This work was supported by Science and Technology Project of State Grid Corporation of China (GY71-14-064 and GC71-14-002).

REFERENCES

[1] Taniguchi S, Okabe S, Asakawa A, et al. Flashover characteristics of long air gaps with negative switching impulses[J]. Dielectrics and Electrical Insulation, IEEE Transactions on, 2008, 15(2): 399-406.

[2] D'Alessandro F, Kossmann C J, Gaivoronsky A S, et al. Experimental study of lightning rods using long sparks in air[J]. Dielectrics and Electrical Insulation, IEEE Transactions on, 2004, 11(4): 638-648.

[3] Yokoyama S. Lightning protection of wind turbine blades[J]. Electric Power Systems Research, 2013, 94: 3-9.

[4] Suzuki T, Miyake K, Kishizima I. Study on experimental simulation of lightning strokes[J]. Power Apparatus and Systems, IEEE Transactions on, 1981 (4): 1703-1711.

[5] Les Renardières Group. Negative Discharges in Long Air Gaps at Les Renardières, 1978 Results[J]. Electra, 1981.

[6] Ortega P, Domens P, Gibert A, et al. Performance of a 16.7 m air rod-plane gap under a negative switching impulse[J]. Journal of Physics D: Applied Physics, 1994, 27(11): 2379.

[7] Taniguchi S, Okabe S. A contribution to the investigation of the shielding effect of transmission line conductors to lightning strikes[J]. Dielectrics and Electrical Insulation, IEEE Transactions on, 2008, 15(3): 710-720.

[8] Li Z, Zeng R, Yu Z, et al. Research on the upward leader emerging from transmission line by laboratory experiments[J]. Electric Power Systems Research, 2013, 94: 64-70.

[9] Zeng R, Wang B, Yu Z, et al. Design and application of an integrated electro-optic sensor for intensive electric field measurement[J]. Dielectrics and Electrical Insulation, IEEE Transactions on, 2011, 18(1): 312-319.

[10] Hidaka K. Progress in Japan of space charge field measurement in gaseous dielectrics using a Pockels sensor[J]. IEEE Electrical Insulation Magazine, 1996, 1(12): 17-28.

[11] Dellera L, Garbagnati E. Lightning stroke simulation by means of the leader progression model. I. Description of the model and evaluation of exposure of free-standing structures[J]. Power Delivery, IEEE Transactions on, 1990, 5(4): 2009-2022.

[12] Larsson A, Bondiou-Clergerie A, Gallimberti I. Numerical modelling of inhibited electrical discharges in air[J]. Journal of Physics D: Applied Physics, 1998, 31(15): 1831-1840.

[13] Wang D, Takagi N, Gamerota W R, et al. Lightning attachment processes of three natural lightning discharges[J]. Journal of Geophysical Research: Atmospheres, 2015, 120(20): 10637-10644.